Article
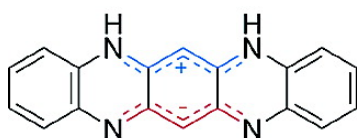
A DFT Study of the Ground State Multiplicities of Linear vs Angular Polyheteroacenes
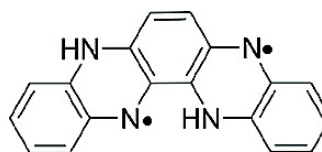
Christos P. Constantinides, Panayiotis A. Koutentis, and Jrgen Schatz

$$\Delta E_{ST} = -10.05 \text{ kcal/mol}$$

$$\Delta E_{ST} = +14.18 \text{ kcal/mol}$$

More About This Article

Additional resources and features associated with this article are available within the HTML version:

- Supporting Information
- Links to the 4 articles that cite this article, as of the time of this article download
- Access to high resolution figures
- Links to articles and content related to this article
- Copyright permission to reproduce figures and/or text from this article

View the Full Text HTML

A DFT Study of the Ground State Multiplicities of Linear vs Angular Polyheteroacenes

Christos P. Constantinides,[†] Panayiotis A. Koutentis,[*,†] and Jürgen Schatz[‡]

Department of Chemistry, University of Cyprus, P.O. Box 20537, 1678 Nicosia, Cyprus, and Division of Organic Chemistry I, University of Ulm, Albert-Einstein-Allee 11, D-89069 Ulm, Germany

Received August 18, 2004; E-mail: koutenti@ucy.ac.cy

Abstract: Unrestricted density functional calculations in combination with the broken-symmetry approach and spin-projection methods have been employed to study a series of formally $4n$ π antiaromatic linear and angular polyheteroacenes. Calculations show that the linear polyheteroacene molecules have either stable singlet zwitterionic **6**−**9** or singlet diradical **5** ground states because they sacrifice the aromaticity of the central arene to form two independent cyanines. The corresponding angular compounds **10**−**14** have robust triplet states, since they cannot create independent cyanines to escape their overall antiaromaticity. An analysis based on the SOMO−SOMO energy splittings, their spatial distributions, and the spin density populations for the triplet states is presented to clarify the factors that determine their ground state multiplicities.

Introduction

During the past two decades, theoretical and experimental studies on molecule-based organic magnets not only have helped in understanding the nature and fundamental principles of magnetism at the atomic level but also have enabled the more effective design and synthesis of organic ferromagnetic materials.[1] Molecule-based magnetic compounds have become a focus in molecular science mainly due to their advantageous properties.[1a,d] Species with unpaired electrons in p orbitals, such as radicals and polyradicals, can be used as spin sources connected through non-Kekulé coupling units to provide possible ferromagnetic compounds.[1b,c] Recently polyheteroacenes were investigated as possible stable heteroatomic diradicals bearing one ferromagnetic coupling unit (*m*-phenylene). Tetraphenylhexaazaanthracene (**1**),[2] an analogue of the stable 1,3-diphenyl-1,2,4-benzotriazinyl radical,[3] and diphenyltetraazapentacene (**2**)[4] were synthesized, characterized, and found to exist as "double-barreled" biscyanine zwitterionic singlets. Analogous biscyanine zwitterionic systems that have since appeared in the literature are the pyridine-bridged bis-1,2,3-dithiazole (**3**)[5] and
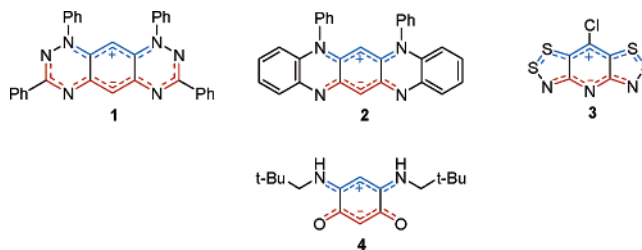

Figure 1. Current family of zwitterionic biscyanine compounds.

the monocyclic 1,2,4,5-tetrasubstituted benzene (**4**).[6] These molecules are the current members of the rapidly growing family of zwitterionic biscyanine compounds (Figure 1).

Recently Braunstein et al. described this family (Figure 1) as "potentially antiaromatic" due to the fact that a single $\pi \rightarrow \pi^*$ excitation would restore π delocalization and antiaromaticity.[6a] To avoid this "potential antiaromaticity" and hence a triplet ground state, the molecules prefer to partition their overall electronic system into two charge conjugated π subsystems (cyanines) which are structurally connected by σ-bonds but not electronically conjugated. Haas and Zilberg[7] indicated that these molecules can be envisioned as the union of two odd electron radicals. These zwitterions are the result of an electron transfer from the donor to the acceptor radical subunit. This transfer will only take place if the donor and acceptor radicals have a low ionization potential and a high electron affinity, respectively.

Calculations, performed on these systems,[2,4−7] indicated that the lowest triplet states of the heterocyclic members of this

[†] University of Cyprus.
[‡] University of Ulm.
(1) (a) Miller, J. S.; Epstein, A. J. *MRS Bull.* **2000**, *25*, 21−28. (b) Veciana, J.; Iwamura, H. *MRS Bull.* **2000**, *25*, 41−51. (c) Rajca, A. *Chem. Rev.* **1994**, *94*, 871−893. (d) Miller, J. S.; Epstein, A. J. *Angew. Chem., Int. Ed. Engl.* **1994**, *33*, 385−415. (e) Crayston, J. A.; Devine, J. N.; Walton, J. C. *Tetrahedron* **2000**, *56*, 7829−7857. (f) Dougherty, D. A. *Acc. Chem. Res.* **1991**, *24*, 88−94. (g) Lahti, P. M. *Magnetic Properties of Organic Materials*; Marcel Dekker: New York, 1999. (h) Miller, J. S. *Inorg. Chem.* **2000**, *39*, 4392−4408. (i) Miller, J. S. *Adv. Mater.* **2002**, *14*, 1105−1110.
(2) Hutchison, K.; Srdanov, G.; Hicks, R.; Yu, H. N.; Wudl, F.; Strassner, T.; Nendel, M.; Houk, K. N. *J. Am. Chem. Soc.* **1998**, *120*, 2989−2990.
(3) Blatter, H. M.; Lukaszewski, H. *Tetrahedron Lett.* **1968**, *22*, 2701−2703.
(4) (a) Wudl, F.; Koutentis, P. A.; Weitz, A.; Ma, B.; Strassner, T.; Houk, K. N.; Khan, S. I. *Pure Appl. Chem.* **1999**, *71*, 295−302. (b) Koutentis, P. A. *Arkivoc* **2002**, *6*, 175−191.
(5) Beer, L.; Oakley, R. T.; Mingie, J. R.; Preuss, K. E.; Taylor, N. J. *J. Am. Chem. Soc.* **2000**, *122*, 7602−7603.

(6) (a) Braunstein, P.; Siri, O.; Taquet, J. P.; Rohmer, M. M.; Bénard M.; Welter, R. *J. Am. Chem. Soc.* **2003**, *125*, 12246−12256. (b) Siri, O.; Braunstein, P. *Chem. Commun.* **2002**, 208−209. (c) Siri, O.; Braunstein, P.; Rohmer, M. M.; Bénard, M.; Welter, R. *J. Am. Chem. Soc.* **2003**, *125*, 13793−13803.
(7) Haas, Y.; Zilberg, S. *J. Am. Chem. Soc.* **2004**, *126*, 8991−8998.

Figure 2. Depicted substitution pattern favors the destabilization of the singlet state.
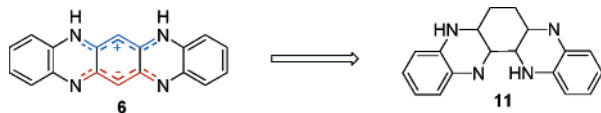
Figure 3. Modification of the linear tetraazapentacene **6** to the corresponding angular structure **11**. The detailed π-structure of the *m*-phenylene coupling unit of molecule **11** is discussed later.

family are energetically close to the singlet zwitterionic ground states, especially for the benzo-bridged bisdithiazole **5**. This close energetic competition can be manipulated within a substitution scheme. Many theoretical and experimental studies on *m*-phenylene diradicals and also on carbenes indicated that substituents can influence their singlet–triplet energy gaps ($\Delta E_{ST} = {}^S E - {}^T E$) and hence their ground state multiplicities.[8] On the basis that the zwitterionic biscyanines can be considered to combine the electronic form of singlet carbenes and the structural motif of *m*-phenylene diradicals, we recently performed a computational study to determine the effects of substituents on the ground state multiplicity of tetraazapentacene **6**.[9] Introduction of electron donating groups (EDG) para to the negative cyanine and electron withdrawing groups (EWG) para to the positive cyanine reduced the ΔE_{ST} in favor of the triplet state. Direct introduction of substituents on the cyanines had a more profound effect on the ground state multiplicity (Figure 2).

A single, direct introduction of an NMe$_2$ group on the central carbon of the tetraazapentacene's negative cyanine led to a drastic reduction of the ΔE_{ST} from -11.4 to -5.5 kcal/mol and revealed the importance of the negative cyanine on the determination of the molecule's ground state multiplicity. A closer look on the geometry of this amino group exposed significant structural differences between the two states. In the singlet state the amino group is out of plane (sum of C–N–C bond angles, 352.1°; torsion angle ϕ, 59.7°), while in the triplet state this group approaches planarity (sum C–N–C bond angles, 360°; torsion angle ϕ, 38.3°). In light of this subtle observation we considered within the context of the present article to modify the structure of the linear tetraazapentacene **6** to an angular form **11**, whereby the tertiary amine is placed directly on the negative cyanine and forced into a planar geometry (Figure 3). This angular structural motif was also applied to other members of the "potentially antiaromatic" family of the biscyanine zwitterions.

The singlet and triplet states of the linear and angular forms of the above compounds (Table 1) were examined using spin

Table 1. Selected Linear (**5**–**9**) and Angular (**10**–**14**) Molecules for the DFT Investigation

molecule	A–B	B–C	C–D	molecule	A–B	B–C	C–D
5	S–S (A–C)		S–N	**10**	S–S (A–C)		S–N
6	NH–CH	benzene fusion	CH–N	**11**	NH–CH	benzene fusion	CH–N
7	NH–CH	CH=CH	CH–N	**12**	NH–CH	CH=CH	CH–N
8	NH–N	N=CH	CH–N	**13**	NH–N	N=CH	CH–N
9	NH$_2$		O	**14**	NH$_2$		O

polarized density functional theory (UDFT). In particular, the hybrid B3LYP method[10] was employed for the computational determination of the spin-coupling constant *J*, which describes the effective exchange interaction between spin-carrier sites and until recently was considered to be an experimental parameter. According to the simple Heitler–London model, the spin-coupling constant *J* can be subdivided into two parameters: (a) the antiferromagnetic contribution βS (β, resonance integral; *S*, quantum integral) which is negative and (b) the ferromagnetic contribution *K* (exchange integral) which is positive.[11] Positive values of *J* result when $\beta S \approx 0$ and $K > 0$ and indicate a parallel alignment of spins in a triplet ground state and hence a ferromagnetic coupling mechanism. Negative values of *J* occur when $\beta S > K$ and designate antiparallel alignment of spins in a singlet ground state and an antiferromagnetic exchange mechanism.

The broken symmetry (BS) approach[8e,f,12,14] was introduced to magnetic coupling by Noodleman[13] and has since been employed to molecular systems bearing possible magnetic exchange interactions (e.g., organic diradicals,[8e,f,12] transition metal complexes,[14] etc.) for the determination of *J*. The BS approach provides lower energies for the singlet states of potential diradicals, which are often spin-contaminated by higher multiplicity states. In contrast triplet states show only a slight spin contamination.[8e,f,12] Spin-projected methods are therefore employed to eliminate the redundant spin contamination from the energy of the BS singlet states; however, these overestimate the stability of the pure singlet states. The true singlet energy

(8) (a) Worthington, S. E.; Cramer, C. J. *J. Phys. Org. Chem.* **1997**, *10*, 755–767. (b) Geise, C. M.; Hadad, C. M. *J. Org. Chem.* **2000**, *65*, 8348–8356. (c) Geise, C. M.; Wang, Y. H.; Mykhaylova, O.; Frink, B. T.; Toscano, J. P.; Hadad, C. M. *J. Org. Chem.* **2002**, *67*, 3079–3088. (d) Shultz, D. A.; Bodnar, S. H.; Lee, H.; Kampf, J. W.; Incarvito, C. D.; Rheingold, A. L. *J. Am. Chem. Soc.* **2002**, *124*, 10054–10061. (e) Zhang, G. B.; Li, S. H.; Jiang, Y. S. *J. Phys. Chem. A* **2003**, *107*, 5573–5582. (f) Zhang, G. B.; Li, S. H.; Jiang, Y. S. *Tetrahedron* **2003**, *59*, 3499–3504.
(9) Constantinides, C. P.; Koutentis, P. A. Effects of substitution on the ground-state multiplicities of zwitterionic polyazaacenes: A DFT study combined with broken symmetry approach. Proceedings of the International Conference on the Science and Technology of Synthetic Metals (ICSM 2004), University of Wollongong, 2004, ISBN 1741280613.

(10) (a) Becke, A. D. *J. Chem. Phys.* **1993**, *98*, 5648–5652. (b) Lee, C. T.; Yang, W. T.; Parr, R. G. *Phys. Rev. B* **1988**, *37*, 785–789.
(11) Kollmar, C.; Kahn, O. *Acc. Chem. Res.* **1993**, *26*, 259–265.
(12) (a) Mitani, M.; Mori, H.; Takano, Y.; Yamaki, D.; Yoshioka, Y.; Yamaguchi, K. *J. Chem. Phys.* **2000**, *113*, 4035–4051. (b) Mitani, M.; Yamaki, D.; Takano, Y.; Kitagawa, Y.; Yoshioka, Y.; Yamaguchi, K. *J. Chem. Phys.* **2000**, *113*, 10486–10504. (c) Mitani, M.; Takano, Y.; Yoshioka, Y.; Yamaguchi, K. *J. Chem. Phys.* **1999**, *111*, 1309–1324. (d) Mitani, M.; Yamaki, D.; Yoshioka, Y.; Yamaguchi, K. *J. Chem. Phys.* **1999**, *111*, 2283–2294. (e) Lahti, P. M.; Ichimura, A. S.; Sanborn, J. A. *J. Phys. Chem. A* **2001**, *105*, 251–260. (f) Illas, F.; de P. R. Moreira, I.; de Graaf, C.; Barone, V. *Theor. Chim. Acta* **2000**, *104*, 265–272. (g) Barone, V.; di Matteo, A.; Mele, F.; de P. R. Moreira, I.; Illas, F. *Chem. Phys. Lett.* **1999**, *302*, 240–248. (h) Barone, V.; Bencini, A.; Ciofini, I.; Daul, C. *J. Phys. Chem. A* **1999**, *103*, 4275–4282.
(13) (a) Noodleman, L. *J. Chem. Phys.* **1981**, *74*, 5737–5743. (b) Norman, J. G.; Ryan, P. B.; Noodleman, L. *J. Am. Chem. Soc.* **1980**, *102*, 4279–4282. (c) Noodleman, L.; Norman, J. G. *J. Chem. Phys.* **1979**, *70*, 4903–4906.

Scheme 1. Spin-Projected Methods Used to Eliminate Spin Contamination

$$J_{ab}^{(1)} = \frac{{}^{SSC}E_{DFT} - {}^{ST}E_{DFT}}{S_{max}^2} \quad \xleftarrow{(A)} \quad J_{ab}^{(3)} = \frac{{}^{SSC}E_{DFT} - {}^{ST}E_{DFT}}{{}^{T}\langle S^2 \rangle - {}^{BS}\langle S^2 \rangle} \quad \xrightarrow{(B)} \quad J_{ab}^{(2)} = \frac{{}^{SSC}E_{DFT} - {}^{ST}E_{DFT}}{S_{max}(S_{max} + 1)}$$

$$^{SSC}E_{DFT} = {}^{SC}E_{DFT} + (ZPE \times SF) \qquad {}^{ST}E_{DFT} = {}^{T}E_{DFT} + (ZPE \times SF)$$

$^{SC}E_{DFT}$ The total energy for the spin-contaminated singlet (BS) state.

$^{SSC}E_{DFT}$ The total scaled energy for the spin-contaminated singlet (BS) state.

$^{T}E_{DFT}$ The total energy for the triplet state.

$^{ST}E_{DFT}$ The total scaled energy for triplet state.

ZPE Zero-point energy

SF Scale factor

$^{X}\langle S^2 \rangle$ The total spin angular momentum for the singlet (BS) and triplet (T) state.

S_{max} The spin size for the triplet state. It comes from $^{T}\langle S^2 \rangle \cong S_{max}(S_{max}+1)$

(A): Weak overlap region $^{BS}\langle S^2 \rangle \cong S_{max} \quad ^{T}\langle S^2 \rangle \cong S_{max}(S_{max}+1)$

(B): Strong overlap region $^{BS}\langle S^2 \rangle \cong 0 \quad ^{T}\langle S^2 \rangle \cong S_{max}(S_{max}+1)$

lies between the spin-contaminated and spin-projected singlet energies in a range of several kcal/mol.[15] Nevertheless, the BS approach is a powerful tool for the qualitative description of the lowest singlet and triplet states of potential diradicals. The three spin-projected methods differ in their application ability, which depends on the degree of overlap between the magnetic orbitals. The first scheme ($J_{ab}^{(1)}$) has been derived by Ginsberg,[16] Noodleman,[13a] and Davidson[17] (GND) and is applied when the overlap of the magnetic orbitals is sufficiently small. The second scheme ($J_{ab}^{(2)}$) has been proposed by GND, Bencini,[18] and Ruiz[19] and is used when the overlap is adequately large. Finally the third scheme ($J_{ab}^{(3)}$) has been developed by Yamaguchi et al.[20] and reduces to the first and second schemes in the weak and strong overlap regions, respectively (Scheme 1).

The energy gap between the pure spin-projected singlet and the UDFT triplets can be estimated as $\Delta E_{ST} = {}^{T}\langle S^2 \rangle J_{ab}$ given by Ginsberg,[16] where $\Delta E_{ST} = {}^{S}E - {}^{T}E$. A positive splitting denotes a triplet ground state. In the results the energies of the unrestricted non-BS singlet states ($^{US}E_{DFT}$) and the corresponding energy gaps of the scaled singlet−triplet states (ΔE_{ST}^{U}) are included for comparison. Where $\Delta E_{ST}^{U} = {}^{SUS}E_{DFT} - {}^{ST}E_{DFT}$

and $^{SUS}E_{DFT}$ = the total scaled energy of the unrestricted non-BS singlet state.

Computational Procedure

The geometries of the singlet and triplet states of molecule **5**−**14** were fully optimized, and analytical second derivatives were computed using vibrational analysis to confirm each stationary point to be a minimum by yielding zero imaginary frequencies at the UB3LYP/6-31G(d) level of theory. The possibility of internal instability in the singlet wave function was investigated using stability calculations. Where instabilities appeared the computations were repeated at the same level of theory using the BS approach. All the energies were corrected after zero-point energies (ZPE) were scaled by 0.981.[21] Furthermore single-point calculations were carried out on the geometries obtained by optimizations, using higher level basis sets: 6-311+G(d,p) and 6-311+G(3df,2p). In these cases zero-point energies were scaled by 0.981 and 0.989, respectively.[21,22] Although molecules **5**,[5] **6**,[4] **8**,[2] and **9**[6] have been previously studied computationally, we repeated the investigation according to our computational methodology. All the above computations were performed using the Gaussian 98 suite of programs.[23]

Results and Discussion

Total Energies, Spin-Coupling Constants, and Singlet−Triplet Gaps. In Table 2, the energies of the singlet and triplet states, the spin-coupling constants (J), and the corresponding

(14) (a) Ciofini, I.; Daul, C. *Coord. Chem. Rev.* **2003**, *238*, 187−209. (b) Onishi, T.; Takano, Y.; Kitagawa, Y.; Kawakami, T.; Yoshioka, Y.; Yamaguchi, K. *Polyhedron* **2001**, *20*, 1177−1184. (c) Takano, Y.; Kubo, S.; Onishi, T.; Isobe, H.; Yoshioka, Y.; Yamaguchi, K. *Chem. Phys. Lett.* **2001**, *335*, 395−403. (d) Takano, Y.; Kitagawa, Y.; Onishi, T.; Yoshioka, Y.; Yamaguchi, K.; Koga, N.; Iwamura, H. *J. Am. Chem. Soc.* **2002**, *124*, 450−461. (e) Onishi, T.; Yamaki, D.; Yamaguchi, K.; Takano, Y. *J. Chem. Phys.* **2003**, *118*, 9747−9761. (f) Sinnecker, S.; Neese, F.; Noodleman, L.; Lubitz, W. *J. Am. Chem. Soc.* **2004**, *126*, 2613−2622. (g) Ren, Q. H.; Chen, Z.; Zhang, L. *Chem. Phys. Lett.* **2002**, *364*, 475−483. (h) Ren, Q. H.; Chen, Z. D.; Ren, J.; Wei, H. Y.; Feng, W. T.; Zhang, L. *J. Phys. Chem. A* **2002**, *106*, 6161−6166. (i) Chen, Z. D.; Xu, Z. T.; Zhang, L.; Yan, F.; Lin, Z. Y. *J. Phys. Chem. A* **2001**, *105*, 9710−9716. (j) Zhang, L.; Chen, Z. D. *Chem. Phys. Lett.* **2001**, *345*, 353−360.
(15) (a) Goldstein, E.; Beno, B.; Houk, K. N. *J. Am. Chem. Soc.* **1996**, *118*, 6036−6043. (b) Yamanaka, S.; Kawakami, T.; Nagao, H.; Yamaguchi, K. *Chem. Phys. Lett.* **1994**, *231*, 25−33.
(16) Ginsberg, A. P. *J. Am. Chem. Soc.* **1980**, *102*, 111−117.
(17) Noodleman, L.; Davidson, E. R. *Chem. Phys.* **1986**, *109*, 131−143.
(18) Bencini, A.; Totti, F.; Daul, C. A.; Doclo, K.; Fantucci, P.; Barone, V. *Inorg. Chem.* **1997**, *36*, 5022−5030.
(19) Ruiz, E.; Cano, J.; Alvarez, S.; Alemany, P. *J. Comput. Chem.* **1999**, *20*, 1391−1400.

(20) (a) Yamaguchi, K.; Jensen, F.; Dorigo, A.; Houk, K. N. *Chem. Phys. Lett.* **1988**, *149*, 537−542. (b) Yamaguchi, K.; Takahara, Y.; Fueno, T.; Houk, K. N. *Theor. Chim. Acta* **1988**, *73*, 337−364.
(21) Scott, A. P.; Radom, L. *J. Phys. Chem.* **1996**, *100*, 16502−16513.
(22) Bauschlicher, C. W.; Partridge, J.; Partridge, H. *J. Chem. Phys.* **1995**, *103*, 1788−1791.
(23) Frisch, M. J.; Trucks, G. W.; Schlegel, H. B.; Scuseria, G. E.; Robb, M. A.; Cheeseman, J. R.; Zakrzewski, V. G.; Montgomery, J. A.; Stratmann, R. E.; Burant, J. C.; Dapprich, S.; Millam, J. M.; Daniels, A. D.; Kudin, K. N.; Strain, M. C.; Farkas, O.; Tomasi, J.; Barone, V.; Cossi, M.; Cammi, R.; Mennucci, B.; Pomelli, C.; Adamo, C.; Clifford, S.; Ochterski, J.; Petersson, G. A.; Ayala, P. Y.; Cui, Q.; Morokuma, K.; Salvador, P.; Dannenberg, J. J.; Malick, D. K.; Rabuck, A. D.; Raghavachari, K.; Foresman, J. B.; Cioslowski, J.; Ortiz, J. V.; Baboul, A. G.; Stefanov, B. B.; Liu, G.; Liashenko, A.; Piskorz, P.; Komaromi, I.; Gomperts, R.; Martin, R. L.; Fox, D. J.; Keith, T.; Al-Laham, M. A.; Peng, C. Y.; Nanayakkara, A.; Challacombe, M.; Gill, P. M. W.; Johnson, B.; Chen, W.; Wong, M. W.; Andres, J. L.; Gonzalez, C.; Head-Gordon, M.; Replogle, E. S.; Pople, J. A. *GAUSSIAN 98*; Gaussian Inc.: Pittsburgh, PA, 1998.

Table 2. Energies (au) of UOS singlet states, BS spin-contaminated singlet states, triplet states, their unscaled zero-point energy (au) corrections, the spin-coupling constants J (kcal/mol) and the corresponding singlet–triplet gaps (kcal/mol) for molecules **5–14**[a]

(A) UB3LYP/6-31G(d) (FOPT)

Molecules	$^{US}E_{DFT}$	ZPE	$^{SC}E_{DFT}$	$^{BS}\langle S^2\rangle$	ZPE	$^{T}E_{DFT}$	$^{T}\langle S^2\rangle$	ZPE	$J^{(1)}$	$\Delta E_{ST}^{(1)}$	$J^{(2)}$	$\Delta E_{ST}^{(2)}$	$J^{(3)}$	$\Delta E_{ST}^{(3)}$	ΔE_{ST}^{U}
5	-1932.02747	0.07142	-1932.03533	0.8138	0.07113	-1932.03561	2.0427	0.07114	0.17	0.34	0.08	0.17	0.14	0.28	5.28
6*	-912.15649	0.26306	Singlet wavefunction stable			-912.13831	2.0482	0.26086	-9.90	-20.27	-4.91	-10.05	-4.91	-10.05	-10.05
7	-604.84194	0.16916	-604.84195	0.0419	0.16866	-604.82279	2.0379	0.16645	-10.53	-21.46	-5.23	-10.66	-5.34	-10.89	-10.35
8	-636.90035	0.14661	Singlet wavefunction stable			-636.87027	2.0334	0.14376	-16.93	-34.43	-8.42	-17.12	-8.42	-17.12	-17.12
9	-492.18071	0.11989	Singlet wavefunction stable			-492.14392	2.0304	0.11749	-21.39	-43.44	-10.64	-21.61	-10.64	-21.61	-21.61
10	-1932.01465	0.07148	-1932.03493	1.0019	0.07135	-1932.04069	2.0397	0.07149	3.48	7.10	1.73	3.53	3.40	6.93	16.33
11*	-912.13146	0.26193	-912.14991	1.0132	0.26151	-912.15419	2.0322	0.26207	2.32	4.71	1.15	2.34	2.30	4.67	14.18
12	-604.81799	0.16830	-604.83605	1.0216	0.16746	-604.83876	2.0275	0.16804	1.33	2.70	0.66	1.34	1.34	2.71	13.20
13	-636.86454	0.14555	-636.88364	1.0165	0.14439	-636.88646	2.0254	0.14513	1.30	2.64	0.65	1.31	1.30	2.64	14.01
14	-492.14763	0.11818	-492.15946	0.9562	0.11710	-492.16639	2.0180	0.11821	3.64	7.35	1.82	3.67	3.45	6.97	11.75

(B) UB3LYP/6-311+G(d,p)//UB3LYP/6-31G(d)

Molecules	$^{US}E_{DFT}$	ZPE	$^{SC}E_{DFT}$	$^{BS}\langle S^2\rangle$	ZPE	$^{T}E_{DFT}$	$^{T}\langle S^2\rangle$	ZPE	$J^{(1)}$	$\Delta E_{ST}^{(1)}$	$J^{(2)}$	$\Delta E_{ST}^{(2)}$	$J^{(3)}$	$\Delta E_{ST}^{(3)}$	ΔE_{ST}^{U}
5	-1932.21810	0.07006	-1932.22455	0.7887	0.06994	-1932.22381	2.0405	0.07010	-0.56	-1.13	-0.28	-0.56	-0.45	-0.92	3.56
7	-605.00180	0.16738	Singlet wavefunction stable			-604.98212	2.0368	0.16512	-10.83	-22.05	-5.38	-10.96	-5.38	-10.96	-10.96
8	-637.06622	0.14515	Singlet wavefunction stable			-637.03566	2.0331	0.14245	-17.33	-35.22	-8.62	-17.52	-8.62	-17.52	-17.52
9	-492.33527	0.11865	Singlet wavefunction stable			-492.29857	2.0281	0.11681	-21.70	-44.00	-10.80	-21.90	-10.80	-21.90	-21.90
10	-1932.20517	0.07025	-1932.22364	0.9983	0.07026	-1932.22892	2.0373	0.07041	3.18	6.48	1.58	3.22	3.10	6.32	14.80
12	-604.97720	0.16686	-604.99568	1.0132	0.16584	-604.99812	2.0266	0.16641	1.17	2.37	0.58	1.18	1.16	2.36	13.40
13	-637.02975	0.14399	-637.04950	1.0054	0.14296	-637.05197	2.0253	0.14369	1.09	2.21	0.54	1.10	1.08	2.19	14.13
14	-492.30742	0.11771	-492.31595	0.9328	0.11656	-492.32174	2.0165	0.11775	2.89	5.82	1.44	2.90	2.68	5.40	8.96

(C) UB3LYP/6-311+G(3df,2p)//UB3LYP/6-31G(d)

Molecules	$^{US}E_{DFT}$	ZPE	$^{SC}E_{DFT}$	$^{BS}\langle S^2\rangle$	ZPE	$^{T}E_{DFT}$	$^{T}\langle S^2\rangle$	ZPE	$J^{(1)}$	$\Delta E_{ST}^{(1)}$	$J^{(2)}$	$\Delta E_{ST}^{(2)}$	$J^{(3)}$	$\Delta E_{ST}^{(3)}$	ΔE_{ST}^{U}
5	-1932.29028	0.07097	-1932.29489	0.7603	0.07083	-1932.29226	2.0404	0.07032	-1.32	-2.69	-0.66	-1.34	-1.04	-2.13	1.64
7	-604.97721	0.16653	Singlet wavefunction stable			-605.02721	2.0365	0.16505	-11.31	-23.04	-5.62	-11.45	-5.62	-11.45	-11.45
8	-637.11457	0.14526	Singlet wavefunction stable			-637.08276	2.0329	0.14248	-18.05	-36.70	-8.98	-18.25	-8.98	-18.25	-18.25
9	-492.37068	0.11916	Singlet wavefunction stable			-492.33237	2.0279	0.11685	-22.41	-45.45	-11.15	-22.62	-11.15	-22.62	-22.62
10	-1932.27464	0.07089	-1932.29268	0.9972	0.07065	-1932.29740	2.0373	0.07065	2.93	5.96	1.45	2.96	2.85	5.80	14.43
12	-605.02188	0.16677	-605.04044	1.0121	0.16604	-605.04287	2.0267	0.16636	1.32	2.67	0.66	1.33	1.31	2.66	13.43
13	-637.07647	0.14385	-637.09642	1.0029	0.14295	-637.09884	2.0255	0.14365	1.08	2.19	0.54	1.09	1.06	2.15	14.16
14	-492.34209	0.11814	-492.34989	0.9313	0.11672	-492.35558	2.0168	0.11793	2.81	5.67	1.40	2.83	2.60	5.25	8.59

[a] (*) denotes the computational expensive single-point calculations of molecules **6** and **11** were not performed.

Table 3. Ground State Dipole Moments (*D*) of Molecules **5**−**14** at the B3LYP/6-31G(d) Level

linear molecules	dipole (*D*)	angular molecules	dipole (*D*)
5	2.73	**10**	1.61
6	7.41	**11**	3.48
7	7.88	**12**	3.85
8	5.07	**13**	3.01
9	8.08	**14**	3.40

Table 4. Energy Difference $\Delta E^X_{ST(L \to A)}$ (kcal/mol) between the Singlet−Triplet Gaps of the Linear and the Corresponding Angular Compounds at the UB3LYP/6-31G(d) Level

linear → angular	$\Delta E^{(3)}_{ST(L \to A)}$	$\Delta E^U_{ST(L \to A)}$
5 → 10	6.65	11.05
6 → 11	14.72	24.23
7 → 12	13.60	23.55
8 → 13	19.76	31.13
9 → 14	28.58	33.36

energy splittings (ΔE_{ST}) for molecules **5**−**14** are tabulated for the full optimizations at the UB3LYP/6-31G(d) level of theory and for the single-point calculations at the higher basis sets 6-311+G(d,p) and 6-311+G(3df,2p), respectively.

The broken symmetry approach is a powerful technique for handling molecules with internal instabilities in their wave functions as, for example, the single states of diradicals.[8e,f,12] The drawback of this method, however, is that the BS solutions of the singlet states are often spin-contaminated by higher multiplicity states. Our calculations for molecules **5**−**14** at the UB3LYP/6-31G(d) level (Table 2a) indicate that the spin contaminations of the triplet states are low and the deviation from the expected value of 2.0 is at most 0.048. In the BS singlet states, the spin contaminations have a broader range of values which span from 0.042 to 1.022. The singlet wave functions of molecules **8** and **9** are free of spin contamination at all the levels of theory. In the case of the linear tetraazaanthracene **7** the spin contamination at the UB3LYP/6-31G(d) level is eliminated when the calculations are performed at the higher basis sets (Table 2b, c). For both the singlet and triplet states of molecules **5**−**14**, the spin contamination is reduced at the higher levels of theory. The spin contamination is approximately the same at the two higher levels of single-point calculations but significantly smaller from the analogous values of the optimizations; e.g., for the angular tetraazaanthracene **12**, the spin contaminations at the 6-311+G(d,p) and 6-311+G(3df,2p) levels are 1.0132 and 1.0121, respectively, while at the 6-31G(d) level it is 1.0216.

The results from the optimization and single-point calculations (*J* and ΔE_{ST}, Table 2) indicated that molecules **6**−**9** and **10**−**14** have singlet and triplet ground states, respectively. All the molecules are $4n$ π antiaromatic systems, and normally triplet ground states would be expected. Experimental and computational studies conducted during the past five years together with the present study indicate that the linear molecules avoid their overall antiaromaticity by accessing a "double-barreled" zwitterionic biscyanine.[2,4−7] Our calculations suggest, however, that the angular molecules **10**−**14** cannot escape their potential antiaromaticity in this manner and thus have triplet ground states.

A consideration of the spin-coupling constants *J* revealed information regarding the ground state multiplicities of molecules **5**−**14**. The linear molecules **6**−**8** have large equally negative spin-coupling constants $J^{(2)}$ and $J^{(3)}$, i.e., a strong overlap region and therefore stable singlet states. The angular molecules **10**−**14** have large equally positive $J^{(1)}$ and $J^{(3)}$ values (weak overlap region) indicating triplet ground states. More information about the ground state nature of these molecules is given by the calculated dipole moments (Table 3).

With the exception of fused dithiazole **5** the linear molecules **6**−**9** have large dipole moments supporting a charge-separated electronic structure. In a previous computational study,[5] molecule **5** was shown to have a triplet ground state of 5.1 kcal/

mol at the B3LYP/6-31G(d,p) level. From Table 2a, the equality of $J^{(1)}$ with $J^{(3)}$ (weak overlap region) along with their small positive values indicated that molecule **5** is a singlet diradical rather than a stable triplet as was first predicted. Moreover according to our calculations at the two higher levels of theory, these coupling constants become marginally negative, due to the stabilization of the singlet state by additive dynamic spin polarization,[24] which causes the violation of Hund's rule.[25] The small dipole moments of the angular molecules **10**−**14** designate, in accordance with the triplet ground state nature described above, that these molecules are not charge-separated species.

The chosen basis sets used in this study can influence the singlet−triplet energy gaps. The ground state dependency of the ΔE_{ST} to the basis sets is, however, small and consistent for most of the molecules. The higher basis sets preferentially stabilize the singlet state giving smaller ΔE_{ST}. This stabilization is greater when the 6-311+G(3df,2p) basis set is used; e.g., for the linear hexaazaanthracene **8**, the change in the $\Delta E^{(3)}_{ST}$ is 0.4 and 1.13 kcal/mol for the 6-311+G(d,p) and 6-311+G(3df,2p) basis set, respectively, in favor of the singlet state. Exceptions to the higher basis sets singlet stabilization trend are the singlet−triplet energy gaps (ΔE^U_{ST}) for molecules **12** and **13** which have slightly bigger values at the two higher levels demonstrating a small stabilization of the triplet states.

The structural modification of the linear compounds into their corresponding angular form has a dramatic change in their singlet−triplet energy gaps and hence in their ground state multiplicities. The differences between the S−T energy gaps of the linear and the corresponding angular compounds ($\Delta E^X_{ST(L \to A)} = \Delta E^X_{ST(A)} - \Delta E^X_{ST(L)}$) at the UB3LYP/6-31G(d) level are listed in Table 4. The biggest change of $\Delta E^{(3)}_{ST(L \to A)}$ (28.58 kcal/mol) is observed in the conversion of **9** (−21.61 kcal/mol) to **14** (+6.97 kcal/mol).

Geometrical Considerations: Bond Order Analysis. The observed geometrical differences in the ground state multiplicities of these two groups of molecules can be easily understood in terms of a bond order analysis. A bond order comparison of the triplet and singlet states of molecules **5**−**9** (Tables S1−S6 in the Supporting Information) supports the "double-barrel" biscyanine structure of these molecules. On going from the triplet to the singlet state of these molecules, the C−N (**5**−**8**), C−S (**5**), C−NH (**6**−**9**), and C−O (**9**) bond orders of the cyanines increase, while the bond orders of the lateral C−C bonds (the bonds which connect the two cyanines) decrease. No significant change in the bond orders of the cyanines C−C bonds was observed. In the singlet states the lateral C−C bonds have bond order values which support their single bond character and therefore the lack of conjugation between the two π

(24) Karafiloglou, P. *J. Chem. Educ.* **1989**, *66*, 816−818.
(25) Borden, W. T.; Iwamura, H.; Berson, J. A. *Acc. Chem. Res.* **1994**, *27*, 109−116.

HOMO   **LUMO**
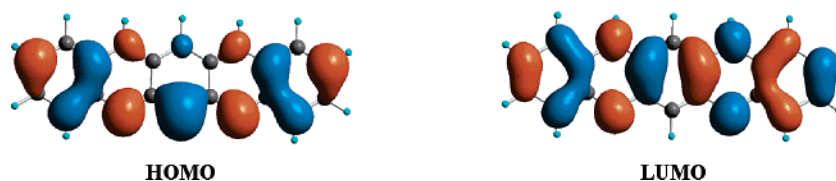
Figure 4. Frontier orbitals of linear tetraazapentacene **6** calculated at the B3LYP/6-31G(d) level with a contour value of 0.02 au and 100×100 grid points.
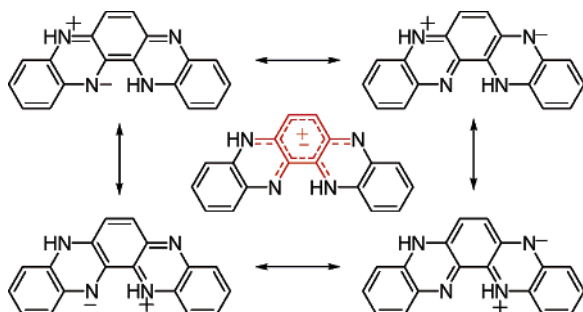
Figure 5. Resonance structures of the angular tetraazapentacene **11**.

subsystems. This shows that molecules **5**−**9** to avoid their overall antiaromaticity prefer to sacrifice the aromaticity of their central benzene ring for the creation of the two independent cyanines. Braunstein explained the above observations using the molecules frontier orbitals (e.g., linear tetraazapentacene **6** in Figure 4).[6a] The delocalized LUMO of these compounds has a large orbital density (π bonding character) over the two lateral C−C bonds of the central benzene ring and nodal points (antibonding character) between the C−N bonds. Promotion of an electron from the HOMO to the LUMO results in the lowest triplet states of these molecules. This electron transfer supplies the C−N bonds and linkage C−C bonds with π-antibonding (smaller bond orders) and π-bonding character (larger bond orders), respectively.

An analogous bond order comparison for the triplet and singlet states of the angular molecules **10**−**14** (Tables S7−S8 in the Supporting Information) revealed that the C−C bond orders of the central benzene ring in these molecules display a moderate uniformity around the value 1.68 ± 0.07, indicating that the aromaticity of the central ring is essentially preserved. From the resonance structures of the angular molecules (e.g., angular tetraazapentacene **11** in Figure 5), it can be seen that they cannot support the electronic partitioning of the "antiaromatic" system into two independent cyanines. The two potential cyanines are electronically connected (cross-conjugated) and overlap over the central benzene ring. The angular molecules **10**−**14** cannot therefore escape from their overall antiaromaticity.

The ground state multiplicity of molecules **5**−**14** is determined by the ability of the molecule to electronically partition into two independent cyanines. The degree of partitioning can be qualitatively measured by considering the aromaticity of the central "sacrificial" arene. For this purpose we have chosen to use Bird's aromatic index[26] (I_A) which is based upon the statistical degree of uniformity of the rings peripheral bond orders, where the aromatic index of benzene is $I_A = 100$ (details on how these indices are calculated are provided in the Supporting Information). The indices of the central rings of the

Table 5. Bird Aromatic Indices (I_A) of the Central Benzene Rings in the Ground States of the Linear Molecules **5**−**9** and Their Angular Analogues **10**−**14**

linear molecule	$I_A{}^l$	angular molecule	$I_A{}^a$
5	54	**10**	74
6	55	**11**	79
7	61	**12**	83
8	56	**13**	85
9	0.5	**14**	55

Table 6. Energy Levels (^1E_S and ^2E_S) and the Energy Gaps (ΔE_{SS}) of the SOMOs for the Triplet States of Molecules **5**−**14** at the B3LYP/6-31G(d) Level

molecule	^1E_S (au)	^2E_S (au)	ΔE_{SS} (eV)	$\Delta E_{ST}^{(3)}$ [a] (kcal/mol)
5	−0.209 06	−0.175 89	0.90	0.28
6	−0.180 48	−0.133 96	1.27	−10.05
7	−0.169 01	−0.120 83	1.31	−10.89
8	−0.211 58	−0.152 79	1.60	−17.12
9	−0.239 43	−0.167 24	1.96	−21.61
10	−0.192 19	−0.183 33	0.24	6.93
11	−0.158 76	−0.146 91	0.32	4.67
12	−0.147 42	−0.134 78	0.34	2.71
13	−0.181 69	−0.169 81	0.32	2.64
14	−0.195 55	−0.179 57	0.43	6.97

[a] The S−T gaps are also listed for comparison.

linear ($I_A{}^l$) and angular ($I_A{}^a$) molecules were calculated (Table 5), and as anticipated the linear molecules **5**−**9** have comparatively smaller aromaticity indicies ($I_A{}^l$ 0.5−61) than their angular counterparts **10**−**14** ($I_A{}^a$ 55−85) supporting the structural deformation of the central aromatic arene on going to a charge-separated system.

In particular the "aromaticity" of the arene in molecule **9** is totally lost ($I_A{}^l = 0.5$) indicating that the separation between the two cyanines is more complete; Braunstein noted[6a] that the lateral C−N bonds of molecule **9** bear mainly σ character. In molecules **5**−**8**, the lateral C−C bonds retain some π-bonding character, and this is reflected by the relatively large aromatic indices ($I_A{}^l \approx 50$).

SOMO−SOMO Energy Splittings: Hoffmann's Postulation. Other factors which influence the ΔE_{ST} and hence the ground state multiplicity of these molecules are the SOMO−SOMO energy splittings (ΔE_{SS}), their topological distributions, and the spin polarization effect. These three factors contribute to the ground state nature of molecules **5**−**14** to varying degrees. According to Hund's rule[27] the ΔE_{ST} should be related to the energy gap of the two SOMOs (ΔE_{SS}). In Table 6, the energy levels (^1E_S and ^2E_S) and energy gaps (ΔE_{SS}) of the two SOMOs of the triplet states of molecules **5**−**14** appear at the B3LYP/6-31G(d) level, since there is no significant difference in these

(26) (a) Bird, C. W. *Tetrahedron* **1985**, *41*, 1409−1414. (b) Bird, C. W. *Tetrahedron* **1987**, *43*, 4725−4730. (c) Bird, C. W. *Tetrahedron* **1992**, *48*, 335−340.

(27) (a) Hund, F. *Linienspekten Periodisches System der Elemente*; Springer-Verlag: Berlin, 1927; p 124ff. (b) Hund, F. *Z. Phys.* **1928**, *51*, 759.
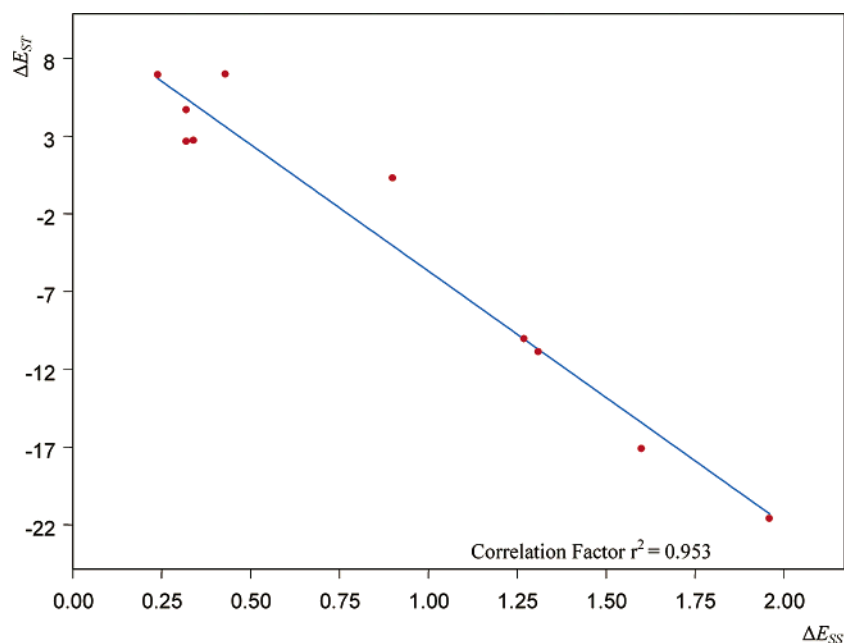
Figure 6. ΔE_{ST} vs ΔE_{SS} for molecules **5–14** at the B3LYP/6-31G(d) level of theory.
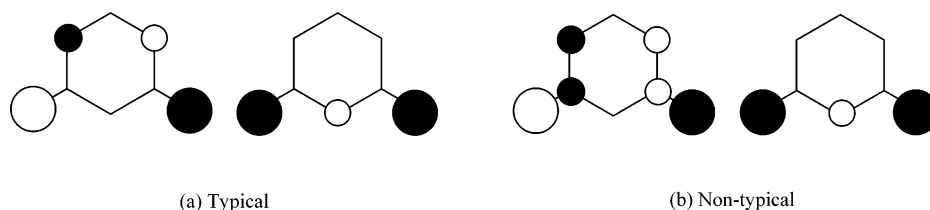

(a) Typical

(b) Non-typical

Figure 7. Nondisjoint SOMOs of *m*-phenylene ferromagnetic coupling unit.

values at the two higher basis sets. Hoffmann[28] provided a rough empirical criterion based on extended Hückel calculations on benzynes and diradicals which suggests that if ΔE_{SS} < 1.5 eV, the two nonbonding electrons will prefer to occupy different degenerate orbitals with a parallel-spin configuration to minimize their electrostatic repulsion leading to a triplet ground state. Based on our calculations, molecules with ΔE_{SS} > 1.3 eV are clear singlets. The linear fused dithiazole **5** which is best described as a singlet diradical has a ΔE_{SS} = 0.9 eV well above the splittings of the triplet molecules **10–14**. These angular molecules **10–14** have very small SOMO–SOMO energy gaps < 0.43 eV (nearly degenerate orbitals) and hence have triplet ground states with large positive singlet–triplet energy gaps (Table 6). From Table 6 and the plot of ΔE_{ST} vs ΔE_{SS} (Figure 6), there is a good linear relationship between the two. Molecules with small ΔE_{SS} splittings tend to have large positive ΔE_{ST}'s, while molecules with large ΔE_{SS}'s have smaller or negative ΔE_{ST}'s.

Shapes of SOMOs: Disjoint, Nondisjoint, and Asymmetrical. The singlet–triplet energy gap of molecules **5–14** is also affected by the spatial distributions of the SOMOs. Borden and Davidson[29] explain that molecules with nondisjoint SOMOs (atoms in common) have a high spin ground state because the

(28) Hoffmann, R.; Zeiss, G. D.; Van Dine, G. W. *J. Am. Chem. Soc.* **1968**, *90*, 1485–1499.
(29) (a) Borden, W. T.; Davidson, E. R. *J. Am. Chem. Soc.* **1977**, *99*, 4587–4594. (b) Borden, W. T. In *Magnetic Properties of Organic Materials*; Lahti, P. M., Ed.; Marcel Dekker: New York, 1999; Chapter 5, pp 61–102.
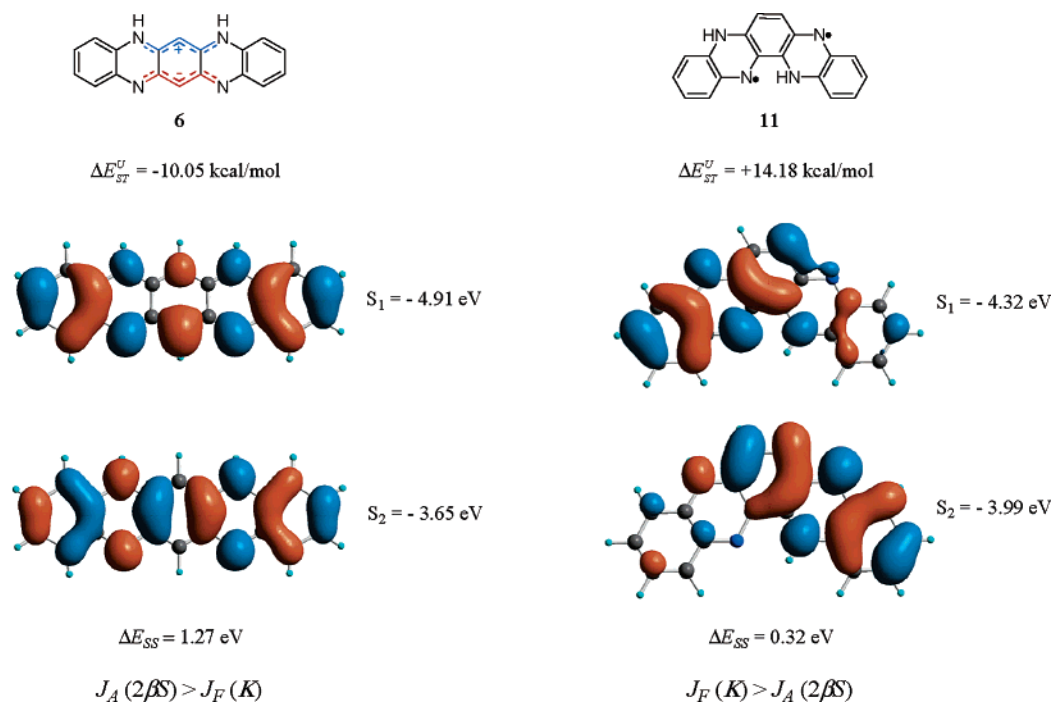
two unpaired electrons cannot appear in the same atomic orbital simultaneously (Pauli forbidden). Molecules with disjoint SOMOs (no atoms in common), however, have at a first approximation singlet and triplet states with similar energies, since the two unpaired electrons can be confined to different sets of atoms (with parallel or antiparallel configurations) to minimize the Coulombic repulsion energy coming from electrons of opposite spin (Pauli allowed). Dynamic spin polarization, in this case, selectively stabilizes the singlet over the triplet state violating Hund's rule and giving rise to singlet diradicals.[25] The disjoint and nondisjoint terminology is based on the connective pattern of two odd radical moieties which join to form a diradical. The nondisjoint SOMOs of the *m*-phenylene ferromagnetic coupling unit, which are sketched in Figure 7, have been called, by Li et al.,[8e] (a) typical and (b) nontypical. Molecules with typical nondisjoint SOMOs have triplet ground states, whereas molecules with nontypical nondisjoint SOMOs were shown to have singlet or near degenerate ground states (singlet diradicals).[8e]

A comparison of the SOMOs of the linear and angular tetraazapentacenes **6** and **11**, respectively, partially explains the observed difference in their ground state multiplicities (Figure 8). The SOMOs of the tetraazapentacene **6** have a large quantum overlap and hence strong antiferromagnetic interaction which leads to a singlet ground state. In contrast the "asymmetrical" SOMOs of molecule **11** have large densities occupying the same region of space. This results in a more intense Pauli exclusion which keeps the two nonbonding electrons from appearing simultaneously in the same region of space. The ferromagnetic

6

$\Delta E_{ST}^{U} = -10.05$ kcal/mol

$S_1 = -4.91$ eV

$S_2 = -3.65$ eV

$\Delta E_{SS} = 1.27$ eV

$J_A (2\beta S) > J_F (K)$

11

$\Delta E_{ST}^{U} = +14.18$ kcal/mol

$S_1 = -4.32$ eV

$S_2 = -3.99$ eV

$\Delta E_{SS} = 0.32$ eV

$J_F (K) > J_A (2\beta S)$

Figure 8. A comparison of the SOMOs of tetraazapentacenes **6** and **11**.

5

7

8

9

10

12

13

14
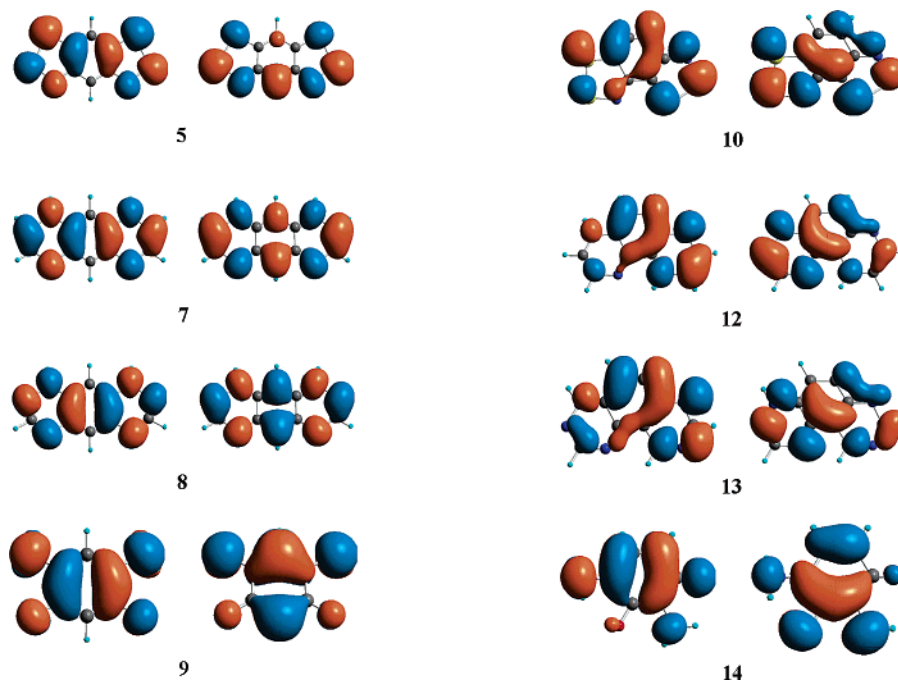
Figure 9. B3LYP/6-31G(d) calculated SOMOs of molecules **5**−**14** pictured with a contour value of 0.02 au and 100 × 100 grid points.
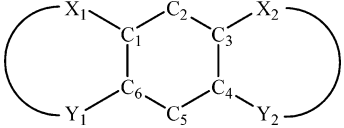
interaction of the two SOMOs maximize the exchange integral *K* and thus the spin-coupling constant leading to a robust triplet.

The linear compounds **5**−**9** which are singlets (**6**−**9**) or singlet biradical (**5**) (Figures 8 and 9) have SOMOs that resemble the nontypical nondisjoint SOMOs of the *m*-phenylene ferromagnetic coupling unit (Figure 7b). The "asymmetrical" SOMOs of the angular compounds **10**−**14** (Figures 8 and 9) do not fit into the two categories of the nondisjoint SOMOs (Figure 7). They could, however, be described as having a nondisjoint character because there is considerable sharing of atomic orbitals, which strongly prevents the two electrons from
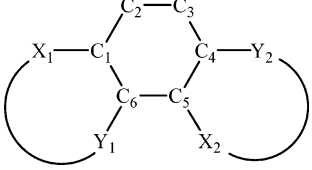
simultaneously appearing in the same region of space giving rise to more stable triplet states.

Spin Densities: Spin Polarization vs Spin Delocalization. Spin delocalization (SD) and spin polarization (SP) are the two mechanisms of spin distribution in *m*-phenylene diradicals. Yamaguchi et al.[12a−d,30] have extensively reported that spin polarization is another source of triplet state stabilization in *m*-phenylene-based diradicals. The SP effect occurs at the

(30) (a) Yamaguchi, K.; Toyoda, Y.; Fueno, T. *Synth. Met.* **1987**, *19*, 81−86. (b) Yamaguchi, K.; Toyoda, Y.; Nakano, M.; Fueno, T. *Synth. Met.* **1987**, *19*, 87−92. (c) Yamaguchi, K.; Okumura, M.; Maki, J.; Noro, T. *Chem. Phys. Lett.* **1993**, *207*, 9−14.

Table 7. Spin Density Populations for the Triplet States of Molecules **5**−**9** Calculated at the UB3LYP/6-31G(d) Level


molecule	atom site									
	X_1	C_1	C_2	C_3	X_2	Y_1	C_6	C_5	C_4	Y_2
5	0.107	0.264	−0.159	0.264	0.107	0.459	−0.174	0.388	−0.174	0.459
6	0.133	0.196	−0.111	0.196	0.133	0.448	−0.114	0.334	−0.114	0.448
7	0.206	0.130	−0.034	0.130	0.206	0.427	−0.079	0.228	−0.079	0.427
8	0.266	0.058	0.038	0.058	0.266	0.365	0.006	0.161	0.006	0.365
9	0.127	0.246	−0.088	0.246	0.127	0.414	−0.049	0.656	−0.049	0.414

Table 8. Spin Density Populations for the Triplet States of Molecules **10**−**14** Calculated at the UB3LYP/6-31G(d) Level

molecule	atom site									
	X_1	C_1	C_2	C_3	C_4	Y_2	Y_1	C_6	C_5	X_2
10	0.136	0.290	−0.156	0.307	−0.162	0.426	0.426	−0.155	0.298	0.156
11	0.164	0.203	−0.071	0.260	−0.094	0.397	0.399	−0.053	0.198	0.188
12	0.216	0.128	−0.019	0.209	−0.066	0.386	0.393	−0.013	0.125	0.228
13	0.270	0.078	0.050	0.141	0.019	0.326	0.339	0.064	0.069	0.285
14	0.197	0.314	−0.025	0.343	−0.006	0.316	0.325	0.006	0.318	0.280

m-phenylene coupling unit via the π-electron system network (Figure 10). The spin of the unpaired electron in the π-orbital polarizes the spins of the paired electrons in the orthogonal σ-orbital in such a way that the two electrons on one atom will have similar spin orientations but opposite from its neighboring atom.

According to theoretical and experimental studies unrestricted DFT is a useful technique for the calculations of spin densities in organic π-radicals.[12a,31] An alternating distribution pattern of spin densities is characteristic for SP and hence of triplet ground states. Furthermore the size of spin densities is directly related to the magnitude of the ΔE_{ST}. Spin delocalization disrupts spin polarization and selectively stabilizes the singlet states. In nontypical nondisjoint diradicals the SP effect is broken down by SD and is responsible for the small ΔE_{ST}.[8e] For molecules **5**−**9**, which were shown above to have SOMOs which resemble the nontypical nondisjoint SOMOs of singlets or singlet diradicals, the SP effect is considerably diminished by the SD mechanism (Table 7). This observation explains partially the singlet ground state nature of these molecules and their small ΔE_{ST}. Normally for molecules **10**−**14**, which were shown to have stable triplet ground states, we would expect an alternating pattern of large spin densities as the SP effect stabilizes the high-spin states. Surprisingly the SP effect, of these molecules, is severely violated by SD (Table 8), especially for the angular hexaazaanthracene **13**. This phenomenon indicates that for the angular molecules **10**−**14** the Coulombic exchange is the main factor which determines their ground state multiplicities. The reduction of the SP effect from SD for molecules **5**−**14** and also for the nontypical nondisjoint diradicals is attributed to the high delocalization character of their SOMOs.

(31) Wright, B. B.; Platz, M. S. *J. Am. Chem. Soc.* **1983**, *105*, 628−630.
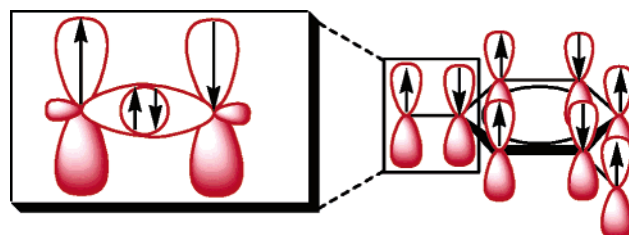
Figure 10. Spin polarization mechanism (through π-network) in *m*-phenylene-based diradicals.

Conclusions

The singlet and triplet states for a series of linear and angular *m*-phenylene-bridged polyheteroacenes have been studied using DFT calculations in combination with the BS approach and spin-projected methods. The calculations show that the linear compounds are either stable zwitterionic singlets (molecules **6**−**9**) or singlet diradicals (molecule **5**), while the corresponding angular analogues are stable triplet diradicals with large singlet−triplet energy gaps. The ground state multiplicity of these molecules is determined by their ability to form independent cyanines. The linear molecules **5**−**9** readily sacrifice the aromaticity of their central benzene ring and access the "double-barreled" biscyanine avoiding in this way their overall antiaromaticity. In contrast the angular molecules **10**−**14** cannot create independent cyanines and cannot escape their antiaromaticity and a triplet ground state. The spatial distributions of the SOMOs are another important factor for the determination of the ground state multiplicity. The SOMOs of the linear molecules **5**−**9** are similar to the nontypical nondisjoint SOMOs of the *m*-phenylene diradicals which are characteristic of stable singlets and singlet diradicals. Their large quantum overlap leads to a strong antiferromagnetic coupling and hence to singlet ground states.

The "asymmetric" SOMOs of the angular molecules **10**−**14**, however, share to a high degree the same atomic orbitals giving rise to a more drastic Pauli prevention and hence to more stable triplet states. The violation of the spin-polarization effect explains the observed ground state multiplicities of the linear compounds but fails to rationalize the triplet ground states of the angular analogues. A better understanding of the origins of the stable triplet states for these compounds **10**−**14** could arise from the use of computationally more demanding methods such as difference dedicated CI (DDCI)[32] that can more accurately predict the magnetic coupling parameters of organic biradicals.

Supporting Information Available: Geometrical data (Tables S1−S8), coordinates, and absolute energies for molecules **5**−**14** at the B3LYP/6-31G(d) level. This material is available free of charge via the Internet at http://pubs.acs.org.

JA045006T

(32) de Graaf, C.; Sousa, C.; de P. R. Moreira, I.; Illas, F. *J. Phys. Chem. A* **2001**, *105*, 11371−11378.